FOGS ON THE YENISEI RIVER, KRASNOYARSK, RUSSIA

by

Nikolai SHAPAREV[a,b], Alexey TOKAREV[a,b*], and Oleg YAKUBAILIK[a,b]

[a]Institute of Computational Modeling, Siberian Branch of the Russian Academy of Sciences, Akademgorodok 50/44, Krasnoyarsk, Russia
[b]Federal Research Center "Krasnoyarsk Science Center of the Siberian Branch of the Russian Academy of Sciences", Akademgorodok 50, Krasnoyarsk, Russia

Original scientific paper
https://doi.org/10.2298/TSCI220402099S

This work presents a study of the formation of cooling and steam fogs on the Yenisei River during 2020. The formation of the above types of fogs resulted from changes in the hydrothermal regime downstream the Krasnoyarsk hydroelectric power station after its construction and it is also associated with a combination of weather conditions and water temperature in the river. Advective cooling fogs form in summer when moist air cools over the surface of cold moving water. The formation of steam fogs in winter, autumn, and spring is associated with the cooling of water vapor above the river surface by cold lower layers of air. The conditions for the formation of fogs are analyzed depending on the air temperature and humidity, water temperature, and wind speed. Based on the remote sensing data, the spatial distribution of steam fogs along the river is determined.

Keywords*: fogs, Yenisei River, downstream, meteorological conditions, water temperature, fog remote sensing*

Introduction

Natural and anthropogenic processes cause the pollution of the Earth's atmosphere. The former ones are natural phenomena associated with sandstorms and volcanic eruptions. Anthropogenic processes are associated with the extraction, processing, and burning of natural raw materials, as well as with forest and agricultural fires. It should also be noted that the regulation of rivers, interfering with their natural regime, can also lead to anthropogenic disturbances of the natural environment. These include, firstly, the formation of fogs, which are a dangerous weather phenomenon. Fog exposure affects aviation; maritime, road and river transport; city buildings; power lines; the environment, and public health.

The study of fog formation relies on observation and simulation. The formation, propagation, and decay of fog result from complex microphysical, thermodynamic, and dynamic processes. Perez-Diaz *et al*. [1] provided an overview of natural fogs regarding their type, forms, and states of occurrence, as well as their physical, microphysical, chemical, and dynamic properties and the main characterizing parameters. The most significant factors which determine the formation of fogs are the following: cooling of moist air due to the divergence of radiative fluxes, mixing of heat and moisture, vegetation, horizontal and vertical winds, heat

*Corresponding author, e-mail: tav@icm.krasn.ru

and moisture transfer in the soil, and horizontal advection and topographic effects [2]. The contribution of each of these factors depends on the location of atmospheric stability and on the season.

The most studied and therefore well-described types of fog are the ones associated with radiation cooling over the land. These can be divided into: radiation fog, high-inversion fog, and advective radiation fog [3]. Mason [4] presented a survey on the physics of radiation fog, including simulation and experimental data. The essence of the phenomenon is the following: on clear nights, the Earth's surface is significantly cooled due to thermal infrared radiation. Subsequently, when interacting with this cooled surface, the lower humid layers of the atmosphere decrease in temperature and turn into fog. The numerical modeling of radiation fog was the subject of research in [5, 6], where various sensitivity tests were carried out to assess the influence of the main input parameters of the model (geostrophic wind, horizontal advection, cloud cover, humidity of the soil) on the predicted fog characteristics. High-inversion fog usually forms in valleys within a deep, wet layer covered with strong inversion [7]. Advective radiation fog is a coastal phenomenon resulting from the radiative cooling of the moist air transported overland from the ocean or any large water body during the previous daylight hours [8].

Another type of fog, the so-called steam fog, occurs as a result of the advection of cold air with the low vapor pressure over a relatively warm water surface and is commonly seen in the Arctic. Due to the difference in vapor pressure between the air and the water surface, there occurs evaporation, and the cooling of the water vapor leads to supersaturation and formation of fog [9-11].

Here we describe a case study of the change in the state of the atmosphere downstream from the Krasnoyarsk hydroelectric power plant (HPP) on the Yenisei River in 2020, caused by the formation of cooling and steam fogs over the moving surface of the river under certain meteorological conditions and at a certain water temperature. It is shown that the advectivity is due to the flow of the river. The spatial distribution of steam fog along the Yenisei River is determined based on the remote sensing data.

Object of research

In terms of the runoff, the Yenisei is the largest river in Russia (599 km^3 per year) and seventh-largest in the world (1.5% of the global runoff) [12]. There are six HPP built in the basin of the river. The Krasnoyarsk HPP, built in 1967, is among the world's ten most powerful HPP (6000 MW) and it is the critical anthropogenic factor influencing the Yenisei River. Upstream, above the dam, a reservoir of 73 km^3 capacity was built, where water cools in wintertime and the surface of the reservoir is covered with ice. In summer, the average water temperature is approximately 20 °C.

Water from this reservoir enters the area downstream the Krasnoyarsk HPP. Depending on the climatic and economic conditions, the water discharge, Q, at the Krasnoyarsk HPP ranges from 2000-8000 m^3 per secunds. The incoming water temperature over the year varies between 2 °C and 12 °C. As a result, downstream of the hydroelectric power station, winter water temperatures are higher, and summer temperatures are lower than before the construction of the Hydropower plant. Therefore, in winter, a polynya forms downstream over a distance of up to 300 km. In summer, the natural temperature regime of the river is restored 700 km away, below the dam. As a result, the hydrothermal regime has changed [13]. The flow speed of the river is $V = Q/S$, where S is the cross-sectional area of the river. The typical values of these parameters are as follows: Q = 3000 m^3/s, S = 2000 m^2, and V = 1.5 m/s.

The thermal regime of the river downstream also contributes to the formation of fogs over the river surface, figs. 1 and 2. Over a distance of 30 km from the dam of the HPP, the river bed is packed between rocky banks that are approximately 400 m high. The resulting fog, confined by these banks, reaches their height and sometimes rises tens of meters higher and slightly beyond the bank. Below the dam, 30 km downstream, there is a valley, where the city of Krasnoyarsk is located. The resulting river fog spreads through this valley and affects the traffic and public health in the city. Our article is devoted to the description of the formation of these fogs.

Figure 1. Steam fog over the Yenisei River (Left bank, January 11, 2020, 11:00)

Figure 2. Cooling fog over the Yenisei River (Right bank, Jul 31, 2020, 7:30)

Instruments and methods

The research sequence was as follows. The formation of fogs was recorded visually and with the help of video surveillance cameras around the clock throughout 2020 (fig. 3, web camera). Next, we analyzed a set of meteorological conditions, which included the meteorological data from monitoring stations (atmospheric pressure, relative humidity, air temperature, wind speed and direction). There are nine monitoring stations located in Krasnoyarsk and its suburbs (fig. 3, Stations 1-9), which automatically measure meteorological parameters at an interval of 20 minutes.

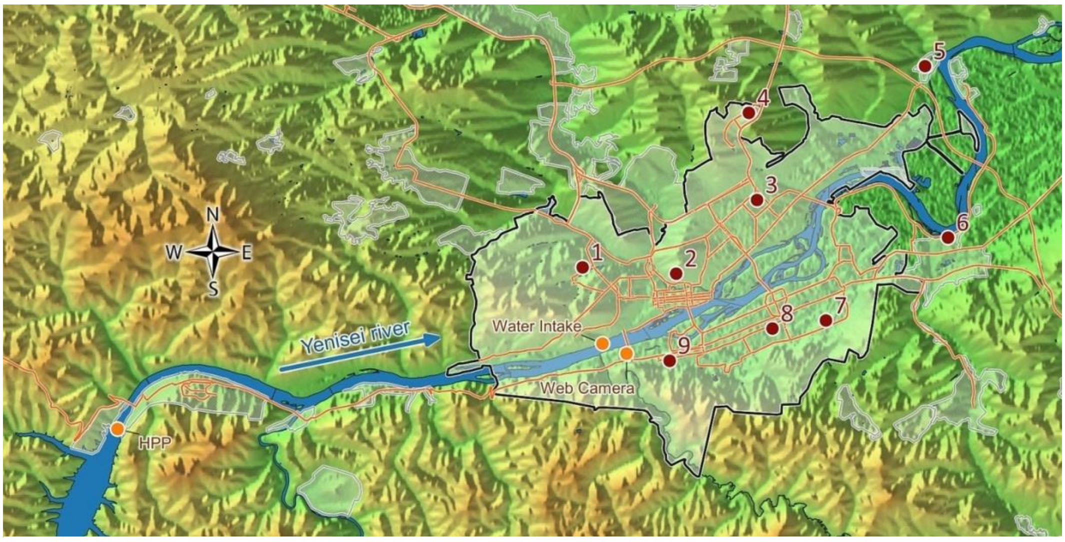

Figure 3. A map of the territory with the marked boundaries of the city, Yenisei River, monitoring stations, HPP, water intake and web camera

The data are automatically transmitted to the Regional Departmental Information and Analytical System of the State of Environment of the Krasnoyarsk Region and then, processed in real time on a geoportal created by the authors [14]. We have developed a Sensor Collector Information System for the scientific research and monitoring of the natural environment in order to help solve the problems of integrating monitoring data from various sources into a centralized database [15]. The system supports the loading, storage, aggregation, automatic calculation of the derived indicators, uploading, and presentation of the data through the web interface. The data sources can be either separate sensors or external databases, or information systems through additional adapters.

The water temperature in the Yenisei River was measured daily at 08:00 at the *Gremyachy Log* water intake, where the width of the river is approximately 600 m (fig. 3, water intake). The analysis of the experimental data from the meteorological observations and water temperature in the river made it possible to determine the type of fog.

In this paper, we also consider the remote sensing data on fogs obtained with a high spatial resolution of 10-30 m per pixel from the Sentinel-2 and Landsat-8 satellites. The analysis of the satellite data shows that such images can reliably determine the location of fogs over the river. Unfortunately, the remote sensing data could not capture all the fogs which occurred, as most of the images are overcast.

Results and discussion

Brief description of fog classification and baseline data for 2020

The formation of fog is due to the condensation of water vapor in the boundary-layer of the atmosphere and river surface, causing low visibility. According to the international classification, cloudiness of the atmosphere is referred to as fog if the atmospheric visibility is lower than 1 km [16].

The main physical parameters of the atmosphere during the fog formation include the relative air humidity and temperature, wind direction and speed, and temperature of the underlying surface next to which fogs are formed. Fogs occur when the relative air humidity becomes saturated due to a drop in the air temperature to the dew point, T_d, or enrichment in water vapor.

Before the Yenisei River was regulated, fogs in Krasnoyarsk were of the radiation, advective, or advective radiation type [17]. Since the construction of the Krasnoyarsk HPP, the situation with the formation of fogs has changed. The hydrothermal regime of the Yenisei River downstream the dam results in lower water temperatures in summer and higher water temperatures in winter as compared with the natural conditions. A new moving underlying surface has thus been created, which facilitates the formation of advective cooling fogs in summer and occurrence of advective steam fogs in winter.

In 2020, fog formation was recorded 45 times. The frequency of fog occurrence during the year is presented in tab. 1. Steam fogs are formed in winter and autumn, while cooling fogs are formed in summer.

Table 1. The monthly distribution of fogs during the year

Year	Month											
	Jan	Feb	Mar	Apr	May	Jun	Jul	Aug	Sep	Oct	Nov	Dec
2020	4	10	2	-	-	-	3	2	11	1	7	5

Advective cooling fogs are formed when the humid air temperature decreases via heat exchange with the cold underlying river surface, without affecting the moisture content in the air. Advective steam fogs arise due to an increase in the temperature and moisture content of the air when interacting with water vapor over the warm underlying surface of the river. A typical picture of the steam fog formation is shown in fig. 1.

Figure 4 shows the seasonal dynamics of water temperature, T_w, in Krasnoyarsk during 2020.

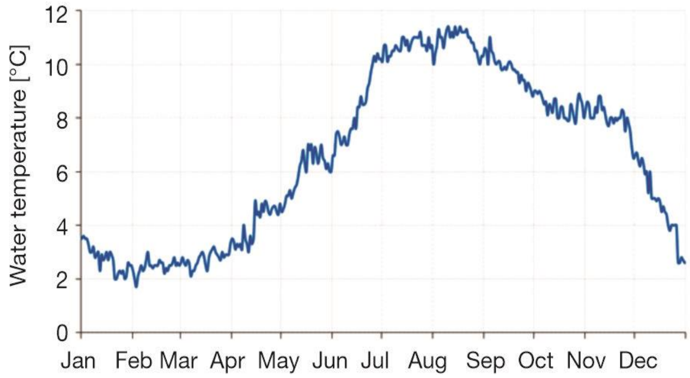

Figure 4. Water temperature in the Yenisei River in 2020

Cooling fogs

Cooling fogs form in warm seasons when the atmospheric temperature, T_a, is higher than the temperature of the underlying water surface, T_w, $T_a > T_w$. This process proceeds as follows. Warm air with a relative humidity of RH < 100% is cooled by advection over a cold underlying water surface. As the temperature reaches the dew point, T_d, the relative humidity (RH) tends towards 100%, and a part of the vapors turns into fog.

The RH is commonly defined as the ratio of the actual water vapor pressure e_a to the saturated vapor pressure e_s:

$$RH = 100\frac{e_a}{e_s} \tag{1}$$

Saturated vapor pressure e_s can be defined by the Magnus–Tetons formula [18]:

$$e_s = b_0 \exp\left(\frac{aT_a}{b+T_a}\right) \tag{2}$$

where b_0 = 6.1094 mbar, a = 17.625, b = 243.04 °C.

The dew point temperature, T_d, is determined by the following formula [19]:

$$T_\mathrm{d} = \frac{bf\left(T_a, RH\right)}{a - f\left(T_a, RH\right)} \tag{3}$$

$$f\left(T_\mathrm{a}, RH\right) = \frac{aT_\mathrm{a}}{b+T_\mathrm{a}} + \ln\left(\frac{RH}{100}\right) \tag{4}$$

The first cooling fog was visually recorded in the evening of July 31 and it dissipated before the lunchtime on August 1, fig. 2. Figure 5 shows the meteorological data averaged over the city of Krasnoyarsk at the time of observation: wind speed (WS), relative air humidity (RH), and air temperature, T_a.

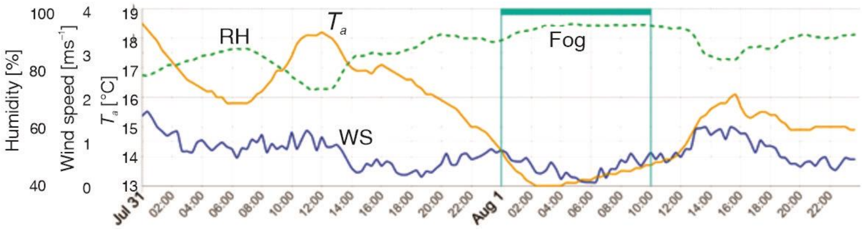

Figure 5. The meteorological data averaged over the monitoring stations for July 31-August 01, 2020

The graphs show that on August 1 at 00:00, the RH increased with the decreasing temperature, T_a, which eventually led to the fog formation. The RH during the fog episode in the coastal zone remained equal to RH ≈ 95%, and the air temperature was T_a = 13-14 °C. For these values (T_a = 13 °C, RH = 95%), according to eq. (3), the dew point temperature is T_d = 12.2 °C. To reach the dew point above the cold surface of the river, a decrease in the air temperature of 0.8 °C is required. In the morning of August 1, the relative humidity subsided as the temperature of the atmosphere, T_a, began to increase, so reaching the dew point, T_d, became impossible, and the formation of fog stopped after 10:00. During the period when the fog was present, there was either no wind or an occasional south-westerly wind at 0.5 m/s. However, the speed of the river flow was 1.5 m/s.

The water temperature during the fog event was equal to T_w = 10.6 °C Thus, in order for the fog to exist, the temperature difference between the air and water has to be lower than $\Delta T = T_\mathrm{a} - T_\mathrm{w}$ = 2.4 °C.

Figure 6 shows the statistical data on the formation of cooling fogs (July-August 2020). Individual points on the diagram represent the averaged values of the meteorological parameters for the specified period with the 1 hour sampling. The data are divided into two series: clear-there is no fog, fog-there is fog. The analysis of the data allows us to conclude that the necessary conditions for fog formation are as follows: the relative humidity RH > 80% and temperature difference 0 °C < ΔT < 6 °C. Beyond these values, the dew point, T_d, is unattainable. At ΔT > 6 °C atmospheric air does not have sufficient time to cool down to the dew point, and, at ΔT = 0 cooling is impossible. In summer, the temperature of water along the river increases and the conditions for the formation of cooling fogs will worsen.

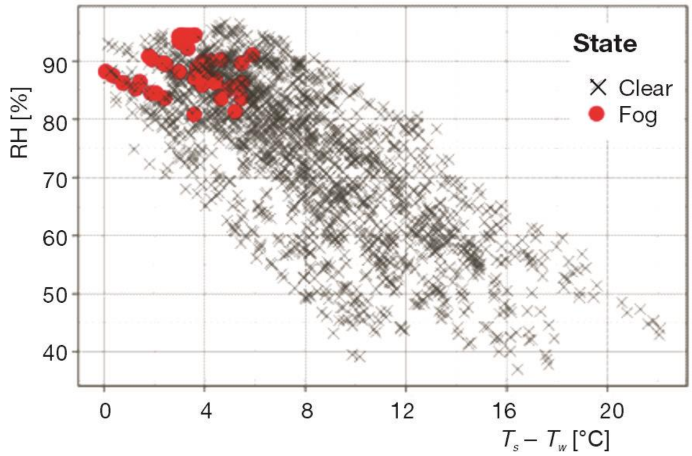

Figure 6. The RH and temperature difference ($\Delta T = T_a - T_w$) during the periods of existence and absence of cooling fog (July, August 2020)

Steam fogs

Steam fogs are formed in winter, early spring, and autumn, when cold atmospheric air comes into contact with a relatively *warm* water surface. The formation of such fogs is due to the steam from the warm surface of the river, followed by cooling of the rising vapors turbulently mixing with the surrounding cold air. In this case, the initial moisture content in the atmospheric air is much lower than that in the atmosphere above the water surface. Fog formation occurs when the temperature of the mixing atmosphere reaches the dew point.

The first steam fog in 2020 formed at 15:00 on January 11 and began to fade after 12:00 on January 12. The movement of the fog was along the course of the river. The averaged meteorological conditions during this period are shown in фig. 7.

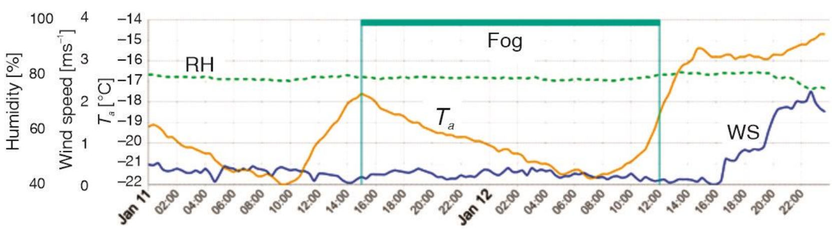

Figure 7. The averaged weather data for January 11–12, 2020

There was no wind during the fog episode. The relative movement of the lower atmosphere and water surface was due to the river current, whose speed was approximately 1.5 m/s. The water temperature in the river was 3 °C at 08:00 on January 11. At the beginning of the fog formation, T_a = –18 °C, RH = 80%. Accordingly, $\Delta T = T_w - T_a$ = 21 °C. Later on, T_a dropped to –21.5 °C, and then increased to –18 °C by the end of the fog event. The relative air humidity during this period remained at 80%. Thus, in order for fog to form and persist, there has to be a certain difference between the water and air temperatures.

Figure 8 presents the statistical data on RH and ($T_w - T_a$) during the existence of steam fogs in 2020, showing the fogs to arise when the temperature difference was in the range of 8 °C < $T_w - T_a$ < 25 °C and RH > 75%.

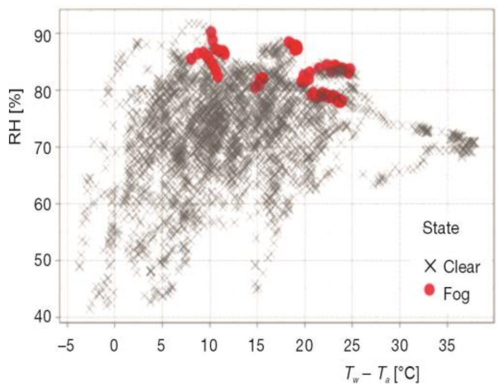

Figure 8. Relative humidity and temperature difference ($T_w - T_a$)_ during the periods of existence and absence of steam fogs (Jan., Feb., Nov., Dec., 2020)

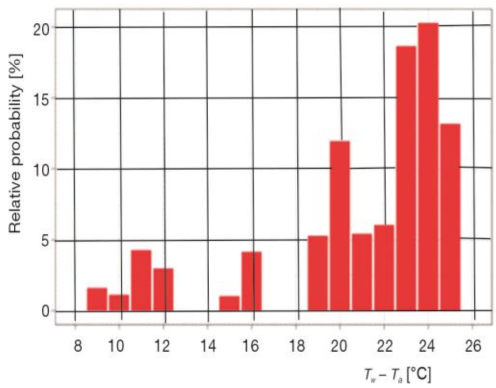

Figure 9. Relative frequency of occurrence of steam fogs depending on the temperature difference $\Delta T = T_w - T_a$ (Jan., Feb., Nov., Dec., 2020)

The relative frequency of fog occurrence depending on the temperature difference is shown in fig. 9. The data show that steam fogs are most likely to form when 20 °C ≤ ΔT ≤ 25 °C

Effect of wind on fog formation

Figure 10 shows the wind speed data during fog events. The analysis of the data shows that, in this situation, the wind speed is lower than 1 m/s. At a higher wind speed, RH does not have time to reach saturation above the surface of the river. Advective processes are mainly associated with the river flow at a speed of approximately 1.5 m/s.

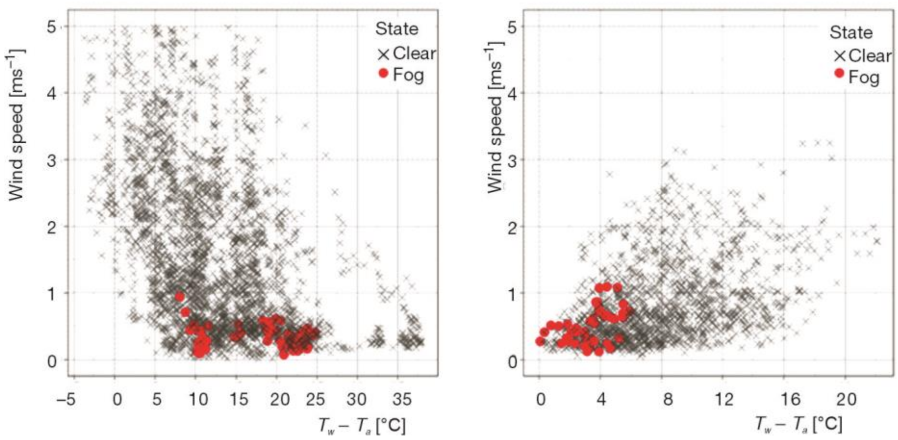

Figure 10. The wind speed; (a) steam fogs (Jan., Feb., Nov., Dec., 2020) and (b) cooling fogs (July, Aug., 2020)

Remote sensing of fogs

The use of satellite information for the fog analysis faces significant technical problems. Fogs are an inconsistent phenomenon. They usually appear at certain times (season of year and time of day) and disappear relatively quickly. Satellite data, in turn, have their spatiotemporal features and time constraints.

Data from satellites of medium spatial resolution (TERRA, AQUA, NOAA-20, and analogs), although capable of providing images several times a day, find little practical application because it is quite a challenge to analyze fogs with transverse dimensions of several hundred meters.

High- and ultra-high-resolution images, with a spatial resolution of 30 meters and higher, can be obtained no more than once every few days, and the shooting is usually performed at around the noon. Another significant problem is cloudiness: for at least half of the year, the sky over Krasnoyarsk is overcast, with clouds making it impossible to use satellite data.

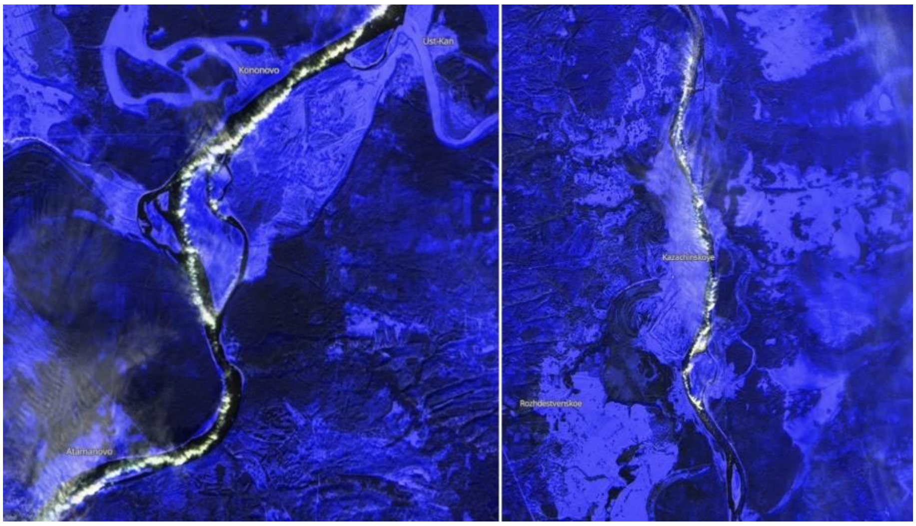

Figure 11. Steam fogs on the Yenisei River; (a) near the village of Kononovo (140 km from the HPP (dam) and (b) near the village of Kazachinskoye (300 km)
The Sentinel-2 satellite image (January 11, 2020, 12:02 local time) is presented in the Urban False Color composite format

The analysis of the satellite data archives from Landsat-8 (15 m spatial resolution of data in the visible range), Sentinel-2 (10 m), Planet Scope (3 m), and Canopus-V (2 m) for the availability of images in which fogs could be detected found only a few scenes in the entire year of 2020 depicting solely steam fogs. In the Sentinel-2 image of January 11, 2020, fig. 11, steam fogs can be observed almost continuously along the Yenisei River section of approximately 200 km in length downstream from the HPP. Further downstream, the fogs are located in separate strata at a distance of up to 300 km. The shooting time corresponds to the onset of fog formation.

In general, the section of the river where steam fogs are formed coincides with the ice-free polynya in winter. Before the Yenisei River was regulated, the river was covered with ice, and therefore there were no steam fogs.

As can be seen in a fragment of the Landsat-8 image acquired on November 28, 2020, fig. 12, as in the previous case, the fog is inhomogeneous and has the form of separate pieces or ribbons. The shooting was performed at the time of the fog dispersion. The meteorological conditions at the time of the satellite imagery acquisition were windless in both cases.

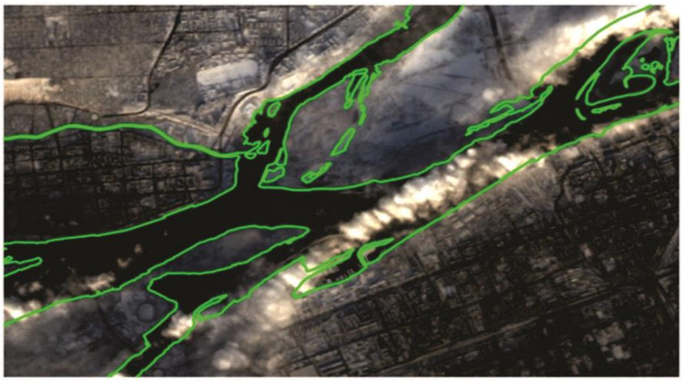

Figure 12. A fragment of the central part of Krasnoyarsk in the Landsat-8 satellite image (November 28, 2020, 11:47 local time), the image in natural colors; the spatial resolution of satellite data in the visible spectral range is 30 meters; the green line indicates the river bank line

.

Influence of the relief and formation of turbulent structures

The orographic features of an area can considerably influence its natural climatic characteristics. In particular, they can be a cause of increased concentrations of pollutants [20], degradation of arable lands and desertification of river valleys [21]. Within this context, it is of interest to estimate the influence of the area relief on fog formation, thus, their possible interconnections are considered in this study.

The dam of the Krasnoyarsk Hydro-Power station is located in an upland area, with its height exceeding 120 meters. As is previously mentioned, the height of the banks of the Yenisei river section from the dam to Krasnoyarsk is 400 meters. The observations of fog formation show that fogs are formed above the river surface; they can reach and even exceed the level of these banks (fig. 1). Near Krasnoyarsk the river width increases, with the river acquiring valley features. However, as in the previous river section, fog is predominantly formed above the water surface and covers the bank line only insignificantly (fig.2). This is also confirmed by the remote sensing data (figs. 11 and 12). The study shows that the key factors of fog formation in the water downstream the Krasnoyarsk Hydro Power Station are the following: the difference in the air and water temperatures, presence of a slight wind with the speed lower than 1 m/s and the river flow rate higher than 1 m/s, these factors provide turbulent heat exchange between the river surface and the humid air medium. Based on the above mentioned it is possible to make a conclusion that the area relief does not influence fog formation.

When considering different approaches to describing the formation and dissipation of fogs one should mention physico-mathematical models involving the description of turbulent processes. The latter ones are the subject of research in different areas, for example, in modeling solvent evaporation in a moving jet of the spinning process [22, 23]. In the problems of describing fog formation above rivers this approach allows modeling wave-like fog patterns along the river accompanied by dissipated whirling columns of fog similar to *steam devils* [24].

These wave-like whirling structures of fog above the river Yenisei can easily be distinguished on the satellite images (fig. 12) and studying their characteristics can be the subject of further investigation.

Conclusions

We registered fogs that occurred over the year 2020 downstream the Krasnoyarsk HPP on the Yenisei River. The total number of fogs in Krasnoyarsk for 2020 was 45. The formation of fogs is due to the anomalous hydrothermal regime downstream of the HPP, which leads to the formation of a moving underlying surface during the year.

It is shown that two types of fog are formed: advective cooling fog in summer and advective steam fog in winter, early spring, and autumn. Advection is caused by a river flow at a speed lower than 1.5 m/s. Fogs are not formed at wind speeds over 1 m/s.

Cooling fogs arise due to a temperature drop in the lower, humid layer of atmospheric air, provided that the relative humidity RH > 80% and the temperature difference between the air and the water is $0\ ^{\circ}\mathrm{C} < T_a - T_w < 6\ ^{\circ}\mathrm{C}$. Steam fogs are formed when water vapor is cooled above the water surface during advection of the river surface with a relatively cold layer of atmospheric air and they are observed at RH > 75% and $8\ ^{\circ}\mathrm{C} < T_w - T_a < 25\ ^{\circ}\mathrm{C}$.

The analysis of the remote sensing data of steam fogs shows that they are formed downstream over a distance of 300 km occupied by a polynya.

References

[1] Perez-Diaz, J. L., *et al*., Fogs: Physical Basis, Characteristic Properties, and Impacts on the Environment and Human Health, *Water (Switzerland), 9* (2017), 10, 807
[2] Duynkerke, P. G., Radiation Fog: A Comparison of Model Simulation with Detailed Observations, *Mon. Weather Rev., 119* (1991), 2, pp. 324-341
[3] Gultepe, I., *et al*., Fog Research: A Review of Past Achievements and Future Perspectives, *Pure Appl. Geophys., 164* (2007), 6-7, pp. 1121-1159
[4] Mason, J., The Physics of Radiation Fog, *J. Meteorol. Soc. Japan. Ser. II, 60* (1982), 1, pp. 486-499
[5] Bergot, T., Guedalia, D., Numerical Forecasting of Radiation Fog. Part I: Numerical Model and Sensitivity Tests, *Mon. Weather Rev., 122* (1994), 6, pp. 1218-1230
[6] Guedalia, D., Bergot, T., Numerical Forecasting of Radiation Fog. Part II: A Comparison of Model Simulation with Several Observed Fog Events, *Mon. Weather Rev., 122* (1994), 6, pp. 1231-1246
[7] Holets, S., Swanson, R. N., High-Inversion Fog Episodes in Central California, *J. Appl. Meteorol., 20* (1981), 8, pp. 890-899
[8] Ryznar, E., Advection-Radiation Fog Near Lake Michigan, *Atmos. Environ., 11* (1977), 5, pp. 427-430
[9] Saunders, P. M., Sea Smoke and Steam Fog, *Q. J. R. Meteorol. Soc., 90* (1964), 384, pp. 156-165
[10] Okland, H., Gotaas, Y., Modelling and Prediction of Steam Fog, *Contributions to Atmospheric Physics, 68* (1995), 2, pp. 121-131
[11] Gultepe, I., *et al*., Turbulent Heat Fluxes Over Leads and Polynyas, and Their Effects on Arctic Clouds During FIRE.ACE: Aircraft Observations for April 1998, *Atmosphere-Ocean, 41* (2003), 1, pp. 15-34
[12] Dingman, S., *Physical Hydrology*, Waveland Press, Long Grove, Ill., USA, 2015
[13] Shaparev, N., Modelling Summer Water Temperature on the Yenisei River, *Thermal Sciences, 23* (2019), Suppl. 2, pp. S607-S614
[14] Shaparev, N., Yakubailik, O., Usage of Web Mapping Systems and Services for Information Support of Regional Management, *MATEC Web Conf., 79* (2016), 01081
[15] Yakubailik, O. E., *et al*., WEB Geographic Information System and the Hardware and Software Ensuring Rapid Assessment of Air Pollution, *Optoelectron. Instrum. Data Process., 54* (2018), 3, pp. 243-249
[16] ***, WMO, Aerodrome Reports and Forecast: A User's Handbook to the Codes, WMO-No. 782, 2020 edition, Geneva, Switzerland, 2020
[17] Shver, C. A., Gerasimova, A. S. *The Climate of Krasnoyarsk*, Hydrometeoizdat: Leningrad, USSR, 1982
[18] Murray, F. W., On the Computation of Saturation Vapor Pressure, *J. Appl. Meteorol., 6* (1967), 1, pp. 203-204

[19] Lawrence, M. G., The Relationship Between Relative Humidity and the Dewpoint Temperature in Moist Air: A Simple Conversion and Applications, *Bull. Am. Meteorol. Soc., 86* (2005), 2, pp. 225-234
[20] Shaparev, N., *et al*., The State of the Atmosphere in the City of Krasnoyarsk (Russia) in Indicators of Sustainable Development, *Int. J. Sustain. Dev. World Ecol., 27* (2020), 4, pp. 349-357
[21] Mei, Y., *et al*., On the Mountain-River-Desert Relation, *Thermal Sciences, 25* (2021), 6B, pp. 4817-4822
[22] Liu, L., *et al*., Dropping in Electrospinning Process: A General Strategy for Fabrication of Microspheres, *Thermal Sciences*, *25* (2021), 2B, pp. 1295-1303
[23] Lin, L., *et al*., Fabrication of PVDF/PES Nanofibers with Unsmooth Fractal Surfaces by Electrospinning: A General Strategy and Formation Mechanism, *Thermal Sciences*, *25* (2021), 2B, pp. 1287-1294
[24] Hrebtov, M., Hanjalić, K., Numerical Study of Winter Diurnal Convection Over the City of Krasnoyarsk: Effects of Non-Freezing River, Undulating Fog And Steam Devils, *Boundary-Layer Meteorol., 163* (2017), 3, pp. 469-495

Paper submitted: April 2, 2022
Paper revised: April 27, 2022
Paper accepted: May 17, 2022